systems

MDPI

Article

Integrated Scheduling of Handling Equipment in Automated Container Terminal Considering Quay Crane Faults

Taoying Li *, Quanyu Dong and Xulei Sun

School of Maritime Economics and Management, Dalian Maritime University, Dalian 116026, China; eiisa_dong.dl@dlmu.edu.cn (Q.D.); xulei_sun@dlmu.edu.cn (X.S.)
* Correspondence: litaoying@dlmu.edu.cn

Abstract: Quay cranes (QCs) play a vital role in automated container terminals (ACTs), and once a QC malfunctions, it will seriously affect the operation efficiency of ships being loaded and unloaded by the QC. In this study, we investigate an integrated scheduling problem of quay cranes (QCs), yard cranes (YCs), and automated guided vehicles (AGVs) under QC faults, which is aimed at minimizing the loading and unloading time by determining the range of adjacent operational QCs of the faulty QCs and reallocating unfinished container handling tasks of QCs. A mixed integer programming model is formulated to dispatch QCs, YCs, and AGVs in ACTs. To solve the model, an adaptive two-stage NSGA-II algorithm is proposed. Numerical experiments show that the proposed algorithm can significantly reduce the impact of faulty QCs on productivity while maintaining its synchronous loading and unloading efficiency. The sensitivity analysis of ship scale, location, and number of faulty QCs indicates that the number of faulty QCs has a greater influence on the loading and unloading efficiency than their locations, and the impact of faulty QCs on the efficiency of small-scale ships is greater than that of large-scale ships.

Keywords: automated container terminal; handling equipment; integrated scheduling; synchronous loading and unloading; quay crane fault

Citation: Li, T.; Dong, Q.; Sun, X. Integrated Scheduling of Handling Equipment in Automated Container Terminal Considering Quay Crane Faults. *Systems* **2024**, *12*, 450. https://doi.org/10.3390/systems12110450

Academic Editor: Wen-Chyuan Chiang

Received: 26 September 2024
Revised: 21 October 2024
Accepted: 24 October 2024
Published: 25 October 2024

1. Introduction

With the rapid development of information technology and increasing global demand for container shipping [1], ACTs have rapidly gained popularity and development due to their advantages of high efficiency [2], low cost, high safety, and environmental protection [3,4]. Meanwhile, the operational efficiency of ACTs largely depends on the reliability of the integrated scheduling system for handling equipment [5,6]. System reliability is inherently linked to the maintenance and performance of critical components. However, as the main equipment in ACTs for loading and unloading containers between container ships and the dock front, once QCs malfunction, they will greatly reduce the reliability of the integrated scheduling system of handling equipment [7].

At present, research on the problem of QC faults can be summarized into three perspectives: the specific types of QC faults, the causes of QC faults, and the rescheduling of QC tasks after the occurrence of faults. This article focuses on the rescheduling of faulty QC tasks during dock loading and unloading processes, and analyzes the impact of the number and location of faulty QC on loading and unloading efficiency for different ship sizes. So, to enhance system reliability and operational efficiency, it is necessary to carry out comprehensive allocation and integrated scheduling of QCs, YCs, and AGVs in ACTs, considering QC faults for efficiency purposes. This proactive approach to maintenance and scheduling not only mitigates the impact of faults but also optimizes the utilization of resources, ensuring the continuous and efficient operation of ACTs [8,9].

Existing solutions for addressing the task scheduling problem of faulty QCs in ACTs can be divided into two categories [10]. One is to reactivate idle QCs or to share the use of

QCs among ships at adjacent berths. However, this solution will increase start-up costs, such as opening, turning on, and warming up, or it may interfere with the operation of the normal QCs adjacent to the faulty ones. Another is to reassign tasks to working QCs that share adjacent berths with faulty QCs by making maximum use of the loading and unloading capacity of the working QCs. This article focuses on the second practical operation scheme.

In this study, a mixed integer programming model is formulated to dispatch QCs, YCs, and AGVs in ACTs, considering QC faults, and an adaptive two-stage NSGA-II algorithm is proposed to tackle the uncertainty of QC faults and solve the integrated scheduling model of handling equipment. Meanwhile, we investigated the impact of ship scale, location and number of faulty QCs on the integrated scheduling efficiency of handling equipment in ACTs. The main contributions of this article are summarized as follows: (1) The task redistribution of both the faulty QCs and their adjacent operational QCs and the integrated scheduling of QCs, AGVs, and YCs are all considered simultaneously in this study; (2) A mixed integer programming model, balancing the processing capacity of working QCs and the overall efficiency of handling equipment, is proposed, which optimizes the task reassignment process of both the faulty QCs and their adjacent operational QCs by minimizing loading and unloading time; (3) An adaptive two-stage NSGA-II algorithm is applied to solve the mixed integer programming problem considering QC faults and numerical experiments reveal that the number of faulty QCs, compared to the location of faulty QCs, has a greater effect on the productivity of ACTs.

The rest of the paper is organized as follows. Section 2 briefly reviews the relevant literature. The problem and model are described in detail in Section 3. The algorithm is designed to solve the problem in Section 4, and numerical experiments are conducted in Section 5. Finally, Section 6 concludes the whole research. The abbreviations and full names mentioned in this article are shown in Table 1.

Table 1. Abbreviation explanation in this article.

Abbreviation	Full Form
QC	Quay crane
YC	Yard crane
ACT	Automated container terminal
AGV	Automated guided vehicle
NSGA-II algorithm	Non-dominated sorting genetic algorithm II

2. Literature Review

The integrated scheduling of handling equipment, including AGVs, QCs, and YCs, is a crucial task of ACTs, which has garnered significant attention from both academics and practitioners [11,12]. As shown in Figure 1, the automated container terminal in this paper takes on a vertical shoreline layout. AGVs transport containers according to route layout and replenishment electricity at charging piles. QCs and YCs pick up containers from AGVs and load them in the correct location. Most of the integrated scheduling problems in the existing literature are achieved through modeling and solving scheduling problems of handling equipment under three loading and unloading modes as shown in Figure 2, which are distinguished by colored lines: blue indicates 'load before unload', black represents 'dual cycle', and orange signifies 'unload before load', respectively. The modeling and solving scheduling problems of handling equipment are actually exploring effective integrated scheduling strategies and their methods, considering various loading and unloading modes.

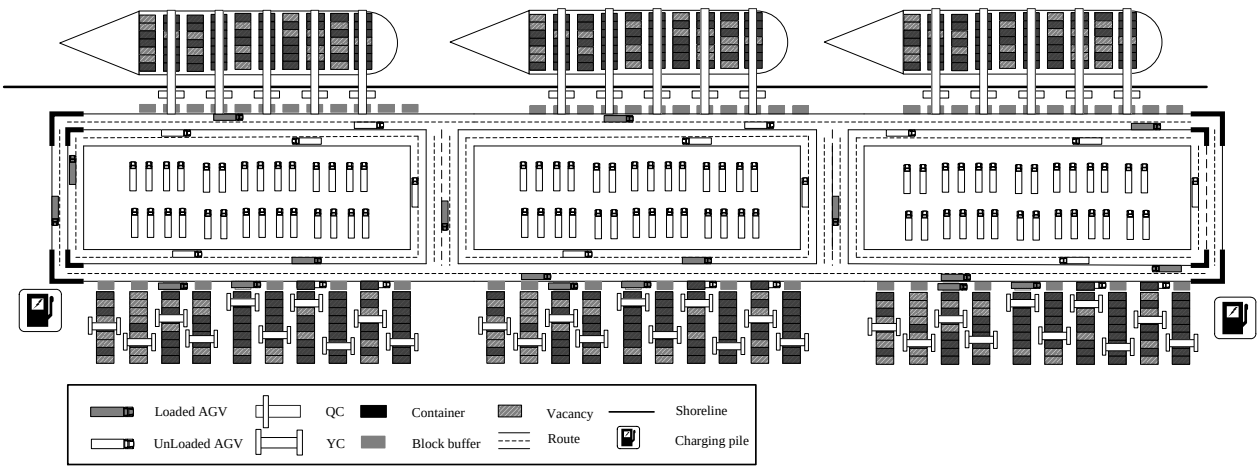

Figure 1. Layout of the automated container terminal.

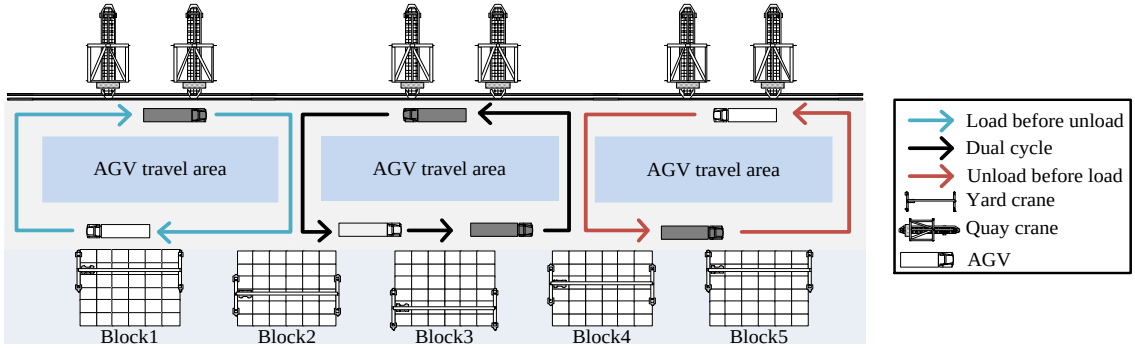

Figure 2. The synchronous and independent loading mode.

Integrated scheduling strategies for handling equipment during loading and unloading processes. Most scholars studying integrated scheduling strategies mainly focus on collaboration and resource allocation of handling equipment in ACTs. For example, Jiang et al. [13] studied the entire coastline integrated scheduling problem of similar QCs and other handling equipment in coastal distribution type ACTs; Tian et al. [14] discussed the integrated scheduling of AGVs and YCs under dual cycling loading and unloading mode; Tan et al. [15] optimized the transport sequence of containers to solve the integrated scheduling problem of loading and unloading equipment; Yang et al. [16] investigated operation process of handling equipment and paid attention to the relationship between efficiency and energy consumption of AGVs. Moreover, some scholars have also taken into account the issue of equipment charging and energy consumption [17–19]. For instance, Li et al. [20] studied the impact of the number of battery packs on the integrated scheduling efficiency of ACTs, and both Xing et al. [21] and Li et al. [22] analyzed the energy consumption of AGVs' different operation behaviors in mixed operation mode.

Methods for solving integrated scheduling optimization problems. It is generally known that the integrated scheduling optimization problem of handling equipment is an NP-hard problem. Most scholars often adopt heuristic algorithms to solve this problem. For example, Klerides et al. [23] proposed a heuristic algorithm with an improved rolling horizon approach to solve the dual-load AGV scheduling problem, and Chen et al. [24] designed a double-layer genetic algorithm to solve and analyze the energy consumption problem of AGVs, considering loading and unloading modes. Huang et al. [25] adopted a large neighborhood search algorithm to solve the container drayage problem in ACTs. In recent years, with the strong rise of deep learning, many scholars consider it an effective solution method due to its ability to solve complex problems. For instance, Xu et al. [26] combined reinforcement learning algorithm and hyper-heuristic genetic algorithm to solve integrated

scheduling optimization of U-shaped automated container terminal. Zheng et al. [27] introduced a deep reinforcement learning approach for information sharing among AGVs to increase the efficiency of automated container terminals. Drungilas et al. [28] solved the integrated scheduling problem of the green automated container terminal, and proposed an AGV speed control algorithm based on deep reinforcement learning to reduce the energy consumption of AGV. Meanwhile, the deep learning algorithm can also be applied to optimize the operation sequence of QCs in the entire coastline [29].

As the main loading and unloading equipment between container ships and AGVs, QCs play a crucial role in the efficiency and service level of ACTs. Once a QC malfunctions, the efficiency of integrated scheduling in ACTs will be severely affected. Thus, the integrated scheduling problem of handling equipment, considering QC faults, has attracted much attention encompassing rescheduling decisions of QCs and uncertainty of QC faults. For instance, Yang et al. [30] investigated the rescheduling problem of loading and unloading operations in the case of sudden QC faults in the ACTs, and Zheng et al. [31] proposed rules for determining the time points of rescheduling decisions while QCs experience faults. Meanwhile, some scholars have proposed a scheduling plan for shared operations of adjacent working QCs [32,33]. Moreover, Zheng et al. [34] considered the uncertainty of QC faults and the diversity of fault scenarios; Chargui et al. [35] established an evaluation model of QC working reliability to calculate the probability of failure; Rajali et al. [36] determined the availability and reliability of QCs using the Stochastic Petri Net to resolve the uncertainty of QC faults.

As mentioned above, most existing research on integrated scheduling of handling equipment and QC faults tends to emphasize the transformation of uncertain issues into deterministic ones and then focuses on optimizing a single problem. However, it ignores the impact of QC faults and various loading and unloading modes on the efficiency of integrated scheduling of handling equipment. Therefore, this article discusses the integrated scheduling problem of handling equipment in ACTs, considering QC faults, by reallocating container handling tasks to adjacent QCs of faulty QCs and minimizing the loading and unloading time.

3. Problem Formulation

This article focuses on the integrated scheduling problem of different handling equipment in ACTs, including QCs, YCs, and AGVs. So, it is essential to develop an overall scheduling plan of a ship for vertical transporting and horizontal transporting containers in order to reduce the total berthing time, which contains location designation and quantity arrangement of import and export containers, the number determination of handling equipment, and the specific task sequence of QCs, YCs, and AGVs. The workflow of handling equipment in ACTs could be divided into four stages, namely ship berthing, unloading, dual cycle, and loading. During the ship berthing stage, the ship will be docked at the designated berth. During the unloading stage, the import containers are first handled from the ship onto AGVs by QCs, and then transported from the quayside to yard blocks by AGVs, and subsequently put into the designated position by YCs. During the dual cycle stage, QCs will pick up import containers from the ship onto AGVs at the same bays after loading export containers from the same AGVs. Containers loaded and unloaded by YCs at corresponding yard blocks and transported by AGVs. During the loading stage, which is the opposite of the unloading stage, YCs unload export containers from yard blocks onto AGVs, and then QCs load export containers from AGVs into the ship.

Nevertheless, considering the uncertainty of QC faults, it is crucial to devise a method for promptly adjusting the integrated scheduling scheme, which mitigates the impact of QC faults on the productivity of handling equipment in ACTs. In this study, we devise a rescheduling mechanism in the optimization model for the unfinished loading and unloading tasks of both the faulty QCs and their adjacent operational QCs. Specifically, when a QC malfunctions, the adjacent operational QCs will assume its incomplete container tasks within the range of several bays. Subsequently, all adjacent operational QCs will

re-optimize their unfinished container tasks, thereby minimizing the impact of the fault on productivity. An improved adaptive Two-stage NSGA-II algorithm is employed to solve the model, with the goal of generating optimal container sequences of loading and unloading tasks based on the fault scenario and maximizing the productivity of the handling equipment. This article first presents the scheme of task assignment under normal operating conditions of QCs and then determines the rescheduling scheme considering the location and number of faulty QCs. Finally, QCs, AGVs, and YCs are assigned based on the overall collaborative optimal task scheduling scheme.

3.1. Assumptions

The following assumptions are proposed to avoid losing generality and ease the modeling process:

- The number of QCs, AGVs, and YCs is known and numbered in sequence;
- Similar handling equipment has the same efficiency;
- Each QC needs to maintain a working distance for operation safety;
- Once a QC faults, the fault information must be obtained immediately and repaired for a fixed amount of time;
- The ship stability, traffic congestion, and AGV collisions during loading and unloading are not considered.

3.2. Model Parameters

The definitions of sets, parameters, non 0–1 variables, and decision variables are presented in Table 2.

Table 2. Notation.

Sets	
M	The set of QCs, $m \in M$
N	The set of YCs, n, $u \in N$
F_f	The set of work stages of QCs, including unloading, dual cycle, and loading, $F_f = \{F_1, F_2, F_3\}$
C	The set of containers, including C_I (the set of import containers) and C_E (the set of export containers)
K	The set of bays, $k \in K$
B	The set of charging piles, $b \in B$
G	The set of AGVs, $g \in G$
Parameters	
C_I^k	The number of import container tasks at bay position k
C_E^k	The number of export container tasks at bay position k
v_1	The travel speed of the AGV unloaded
v_2	The travel speed of the AGV overloaded
b_g^0	The initial power of the AGV g
b'	The battery per unit time of AGV consumption
b''	The battery per unit time of AGV charging
S_m^s	The initial position of QC m during the course of a loading and unloading operation
S_m^a	The position of other QCs adjacent to QC m, including S_m^l (the left of m) and S_m^r (the right of m)
$C\_$	The safe power of AGV completing the transporting task of container
t_1	The unit time of a QC handling a container in single cycle (loading or unloading) mode
t_2	The unit time of a QC handling containers in dual cycling mode
t_3	The unit time of a YC handling a container
t_*	The unit time of a YC flipping a container
S_{ik}	The specific bay position of the container i

Table 2. *Cont.*

Non 0–1 variables	
b_{gi}	The current charge of AGV g after completing the transporting task of container i
l_{mn}	The distance between QC m and YC n
l'_{nu}	The distance between YCs n and u
l''_{bn}	The distance between the charging pile b and the YC n
l'''_{bm}	The distance between the charging pile b and the QC m
p_i	The number of containers above container i
t^{QC}_{im}	The moment when QC m starts loading and unloading the container i
t^{YC}_{in}	The moment when YC n starts loading and unloading the container i
Non 0–1 variables	
Z^k_m	The number of tasks for QC m to load and unload containers at bay k
t^b_g	The total time of AGV g charging during the course of transporting task
t^{QC}_{gm}	The total time of QC m handling containers for AGV g
$\hat{t}^{mn}_g$	The total time of AGV g transporting containers from QC m to YC n at single cycle model
$\dot{t}^{nm}_g$	The total time of AGV g unloaded from YC n to QC m at single cycle model
t^{YC}_{gn}	The total time of YC n handling containers for AGV g
$\tilde{t}^{nu}_g$	The total time of AGV g unloaded traveling between YCs n and u
$\ddot{t}^{nm}_g$	The total time of AGV g transporting containers from YC n to QC m at dual cycle model
Decision variables	
ω^k_m	The state of the QC m, $\omega^k_m =$ 1, if QC m works normally at the bay k, otherwise $\omega^k_m = 0$
c_{gi}	$c_{gi} = 1$, if $b_{gi} < C_-$, AGV g needs to be charged, otherwise $c_{gi} = 0$
θ^m_{ij}	$\theta^m_{ij} =$ 1, if the QC m carries container j after completing container i, otherwise $\theta^m_{ij} = 0$
o^k_{mi}	$o^k_{mi} = 1$, if containers i of bay k is assigned to the QC m, otherwise $o^k_{mi} = 0$
δ_{im}	$\delta_{im} = 1$, if the QC m carries container i, otherwise $\delta_{im} = 0$
ε_{ig}	$\varepsilon_{ig} = 1$, if the AGV g carries container i, otherwise $\varepsilon_{ig} = 0$
γ_{in}	$\gamma_{in} = 1$, if the YC n carries container i, otherwise $\gamma_{in} = 0$
x^g_{ij}	$x^g_{ij} =$ 1, if the AGV g carries container j after completing container i, otherwise $x^g_{ij} = 0$

3.3. Mathematical Model

The above assumptions and parameters are considered to build the integrated scheduling model of handling equipment in ACTs considering QC faults, which redistributes the task of both the faulty QCs and their adjacent operational QCs, and synchronously optimizes the task assignment of handling equipment, namely QCs, AGVs, and YCs. The overall goal of maximizing the efficiency of ACTs is realized through a globally optimal strategy, which is idealized to minimize the maximum AGV task completion time. The detailed optimization model is as follows.

Obj.

$$T = \min_{g \in G} \max \sum\nolimits_{m \in M} \sum\nolimits_{n,u \in N} \left(t^{QC}_{gm} + \hat{t}^{mn}_g + t^{YC}_{gn} + \tilde{t}^{nu}_g + \dot{t}^{nm}_g + \ddot{t}^{nm}_g + t^b_g \right) \tag{1}$$

S.t.

$$\sum\nolimits_{f=1}^{3} F_f = 1 \tag{2}$$

$$|S^s_m - S^a_m| \geq 2 \tag{3}$$

$$|S^s_m - S_{ik}| < \left| S^s_m - S_{jk} \right|, \forall i, j \in C, i \neq j, \forall k \in K, o^k_{mi} = 1 \tag{4}$$

$$Z_m^k = \sum_{i=1}^{C} \sum_{j=1}^{C} o_{mi}^k \times \omega_m^k \left(1 - \theta_{ij}^m\right), \forall k \in K \tag{5}$$

$$\frac{C_E^k + C_I^k - 1}{2} \leq \sum_{m \in M} Z_m^k \leq C_E^k + C_I^k \tag{6}$$

$$\sum_j \theta_{ij}^m \leq 1, \forall i, j \in C \tag{7}$$

$$\sum_i \theta_{ij}^m \leq 1, \forall i, j \in C \tag{8}$$

$$t_{im}^{QC} < t_{jm}^{QC}, \forall i \in C_E, \forall j \in C_I, \theta_{ij}^m = 1 \tag{9}$$

$$t_{in}^{YC} < t_{jn}^{YC}, \forall i \in C_I, \forall j \in C_E, x_{ij}^g = 1 \tag{10}$$

$$t_{gm}^{QC} = \sum_{i=1}^{C} \varepsilon_{ig} \times \delta_{im} \times \left[\left(1 - \theta_{ij}^m\right) \times t_1 + \theta_{ij}^m \times t_2\right] \tag{11}$$

$$t_{gn}^{YC} = \sum_{i=1}^{C} \varepsilon_{ig} \times \gamma_{in} \times (t_3 + 2p_i \times t_*) \tag{12}$$

$$\sum_{g \in G} \varepsilon_{ig} \leq 1, \forall i \in C \tag{13}$$

$$\sum_{i \in C} x_{ij}^g \leq 1, \forall j \in C \tag{14}$$

$$\sum_{j \in C} x_{ij}^g \leq 1, \forall i \in C \tag{15}$$

$$\hat{t}_g^{mn} = \sum_{m \in M, n \in N} \sum_{i=1}^{C_I} \varepsilon_{ig} \times l_{mn} / v_2 \tag{16}$$

$$\ddot{t}_g^{nm} = \sum_{m \in M, n \in N} \sum_{i=1}^{C_E} \varepsilon_{ig} \times l_{nm} / v_2 \tag{17}$$

$$\tilde{t}_g^{nu} = \sum_{n,u \in N} \sum_{i,j \in C} x_{ij}^g \times l'_{nu} / v_1 \tag{18}$$

$$\dot{t}_g^{nm} = \sum_{m \in M, n \in N} \sum_{i=1}^{C} (1 - c_{gi}) l_{nm} / v_1 \tag{19}$$

$$b_{gi} = b_g^0 - b' \times l \tag{20}$$

$$t_g^b = \sum_{i=1}^{C} c_{gi} \times \left\{ \frac{l''_{bn}}{v_1} + \frac{b' \times l}{b''} + \frac{\left[F_1 \times l'''_{bm} + (F_2 + F_3) \times l''_{bn}\right]}{v_1} \right\} \tag{21}$$

Constraint (2) means the current work stages of QCs; Constraint (3) means that the safe operating distance is less than two bays; Constraint (4) represents that container *i* is assigned to the QC with the shortest moving distance; Constraint (5) is the sum of tasks of QC m at bay *k*; Constraints (6) represents the range of the task number of bay *k*; Constraints (7) and (8) ensure that any container has no more than one preceding task; Constraint (9) and (10) means the sequence of tasks of the QCs and YCs; Constraints (11) and (12) denote the total working time of QCs and YCs for AGV *g*; Constraints (13)–(15) express the sequence of tasks of AGVs; Constraints (16)–(19) denote the total time of each stage of AGVs in different loading and unloading modes; Constraints (20) indicates the energy consumption of AGVs; Constraint (21) represents the sum of the AGV charging time.

4. Solution Approach

The transportation of import and export containers in ACTs requires a variety of handling equipment (such as QCs, AGVs, and YCs) to cooperate closely between the terminal and the yard blocks. Therefore, the integrated scheduling of handling equipment in ACTs is an NP-hard problem expressed as a mixed integer programming (MIP) model. Since the NP-hard problem is difficult to obtain the exact solution in a limited time [37], more and more researchers use heuristic algorithms to gradually approximate the optimal solution [38]. For example, Li et al. [39] proposed a hybrid evolutionary algorithm by combining non-dominated sorting genetic algorithm II (NSGA-II) and local search method; Chen et al. [40] combined Convolutional Neural Network (CNN) and the Deep Determinis-

tic Policy Gradient (DDPG) algorithm to solve time and space synchronization scheduling problem of handling equipment; and Ji et al. [41] also considered AGV conflict-free routing during integrated scheduling.

In order to efficiently address task redistribution of both the faulty QCs and their adjacent operational QCs and optimize the task assignments of handling equipment, based on the logical relationship among QCs, YCs, and AGVs in ACTs, this paper constructs an adaptive two-stage NSGA-II algorithm for solving the mixed integer programming model. The proposed algorithm focuses on the allocation and optimization of handling equipment in ACTs, determines the container loading and unloading sequences of QCs, AGVs, and YCs according to specific fault scenarios, and finally obtains the global optimal solution through adaptive dynamic adjustment, whose detailed process is shown in Figure 3 and pseudo-code is displayed as Algorithm 1.

Algorithm 1: Two-Stage NSGA-II algorithm for integrated scheduling of transport equipment

This Two-Stage NSGA-II algorithm is divided into three parts: a, b, and c.
Initialization: Location of import and export containers. Randomly generate container sequences.
Algorithm a:
  Input: import container sequence $(Q = \{1, 2, \cdots, q\})$
    /* Genetic algorithm */
    for generation $= \{1, \cdots, 100\}$ ***do***
      Sort the top 10 sequences are selected based on fitness $(1/T)$
      for population size $= \{1, \cdots, 50 - 10\}$ ***do***
        if the random number < crossover probability ***then***
          The new seq = crosses the sequence population $[i]$
        for $i = \{10, \cdots,$ populationsize$\}$ ***do***
          if the random number < variation probability ***then***
            Mutate new_seq
      Renewal population
  Output: import container handling sequence with maximizing fitness
Algorithm b:
  Input: import container handling sequence from algorithm a
    Randomly generated population of import container handling sequence
    for generation $= \{1, \cdots, 100\}$ ***do***
      Calculate fitness for each sequence by genetic algorithm
  Output: export container handling sequence with maximizing fitness
Algorithm c:
  Input: import and export container handling sequence from algorithms a and b
    for generation $= \{1, \cdots, 100\}$ ***do***
      Obtain new sequence by genetic algorithm
      Calculate the fitness function
  Output: import and export container handling sequence with maximizing fitness
Output: import and export container handling sequence with maximizing fitness from memory
end

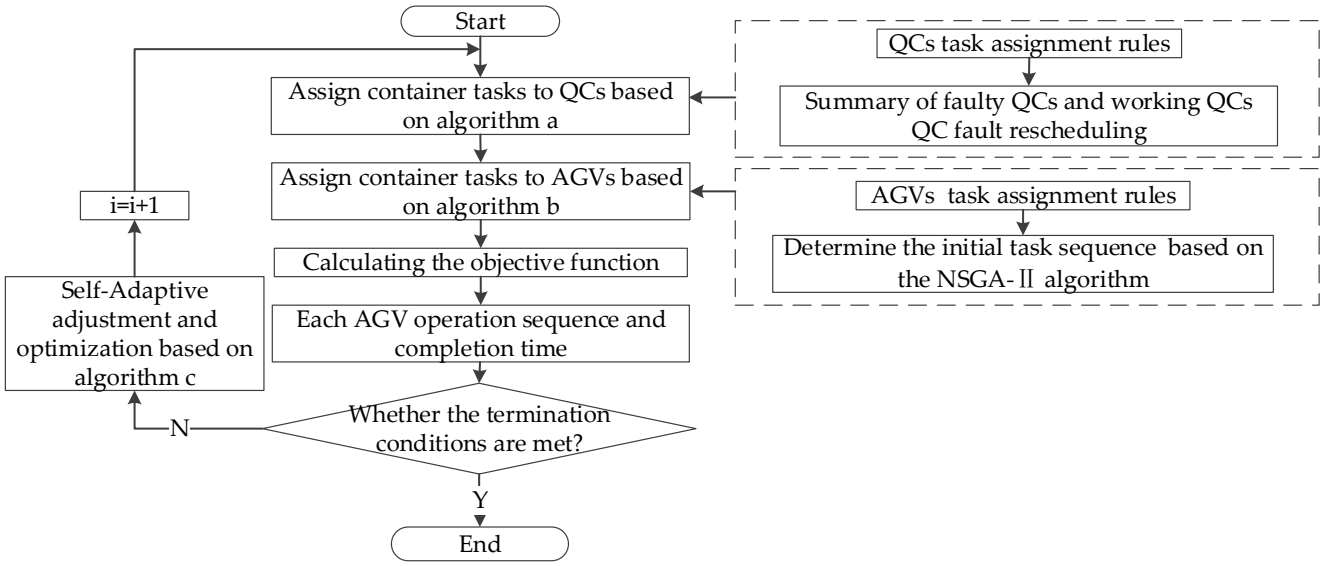

Figure 3. Flowchart of two-stage NSGA-II algorithm.

4.1. Chromosome Representation and Fitness Evaluation

Among many coding methods, permutation encoding can express the task sequence more intuitively and conveniently, and real-valued encoding can directly generate the genes of new individuals in the process of crossover and mutation, which makes it easier to generate feasible solutions. To distinguish tasks of QCs, AGVs, and YCs, and clearly represent the sequence of tasks involved during the process of container loading and unloading, a hybrid encoding method is employed to integrate permutation encoding and real-valued encoding. Specifically, each chromosome represents an orderly loading and unloading sequence scheme, and each gene expresses a specific task sequence. The first line in Figure 4 shows the sequence of container tasks, where positive numbers show import containers and negative numbers denote export containers. The second, third, and fourth lines indicate the allocation of QCs, AGVs, and YCs for the completion of the corresponding assigned tasks.

Task Sequences	-8	2	-3	10	-5	7	-1	-6	9	-4	-2	6	-9	3	-7	5	-10	8	1	7
QC	2	4	3	1	4	2	3	1	2	4	3	1	3	2	4	1	4	2	3	1
AGV	5	2	3	1	4	6	2	1	4	3	6	5	1	2	4	3	6	5	1	2
YC	2	1	3	2	1	3	1	3	2	3	1	2	2	3	1	2	3	1	2	1

Scheduling rules determine the sequence of tasks

Figure 4. Schematic diagram of chromosome operation.

Based on the planned operation sequence of containers, a task sequence is generated for the QCs, AGVs, and YCs while considering scheduling constraints. The objective function T aims to minimize the maximum completion time of tasks of AGV, and the fitness function is expressed as the reciprocal of T.

4.2. Parent Selection Strategy

In order to quickly find the optimal solution, the elite strategy is used for the selection operation. Specifically, the 50 individuals in the population are sorted according to their fitness value, and the top 10 individuals are selected. This strategy is able to improve the quality of the initial population solutions and speed up the convergence of the algorithm.

4.3. Crossover Operation

The crossover operation selects two parents randomly from the top 10 ranked parents. A crossover point is also randomly selected, and then the genes of the other parent are traversed to exclude the gene sequence before the crossover point of the parent with higher

fitness in the pair. As shown in Figure 5a, the new individual's gene is composed of the gene sequence of one parent before the crossover point and the remaining non-repeating gene sequence of another parent. This method can effectively avoid the problem of generating an infeasible gene sequence by crossover, reducing the steps of gene repair and solution space cutting, and reducing the algorithm's time complexity.

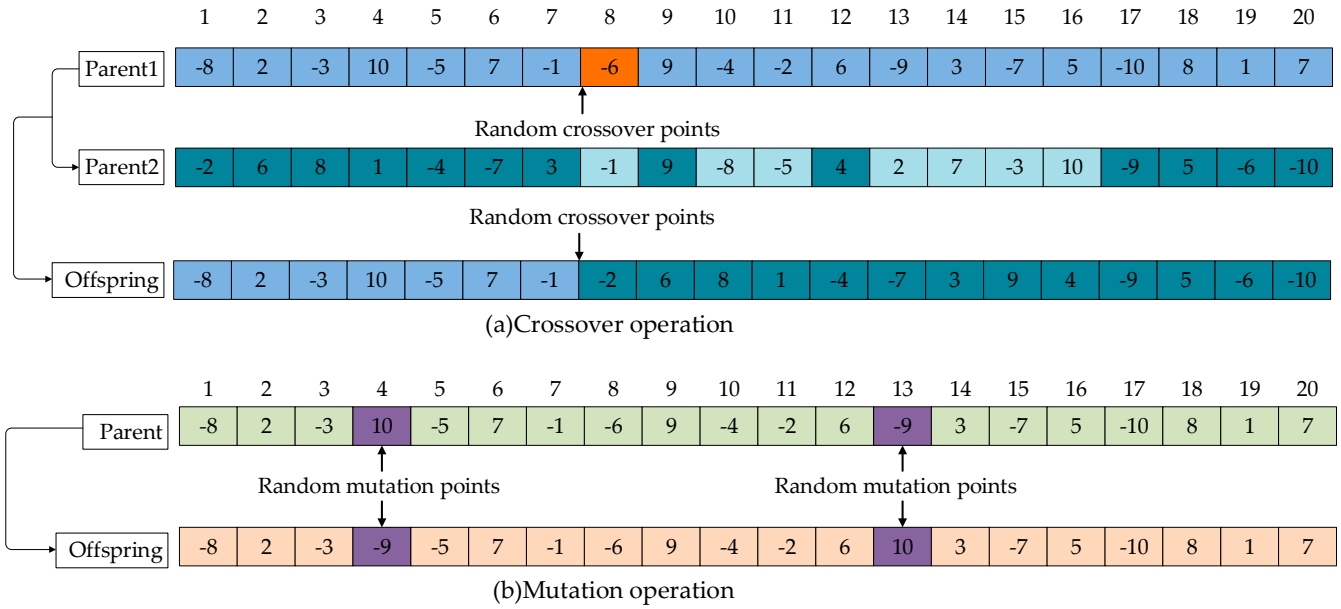

Figure 5. Crossover and mutation operations.

4.4. Mutation Operation

The 40 new offspring individuals generated by the crossover operation are subjected to gene mutation operation. Random selection mutation is used, and the mutation probability is set to 0.1. The individual with the mutation randomly selects two positions on the gene and exchanges their values. As shown in Figure 5b, the random gene positions of the mutated offspring generated by crossover are 4 and 13, and their positions are exchanged to generate new offspring.

5. Numerical Experiment and Discussion

The article analyzes how the health status of the QCs and the dual cycling model can affect the loading and unloading efficiency of container ships in ACTs. In this section, we carry out experimental analysis using a ship as a case, and five different combinations of location and number of faulty QCs are considered based on the scales of different container ships. The experiment considered dividing three real ship scale scenarios based on ship length and container quantity, referring to existing literature and ship length data provided by Chinese ship websites https://www.chinaports.com/. Numerical analysis is conducted to evaluate the effectiveness of the two-stage NSGA-II algorithm and demonstrates the superiority of task rescheduling and dual cycling loading and unloading strategies under QC faults.

In order to express the experimental scenario mentioned in this section more clearly, take three QC responsible for loading and unloading a container ship with a length of 10 bays as an example. As shown in Figure 6, the tasks of loading and unloading containers for QC "a" and "c" before and after the fault of QC "b" located in the middle have been rescheduled, sharing container tasks 30 and 38 for QC "b", respectively.

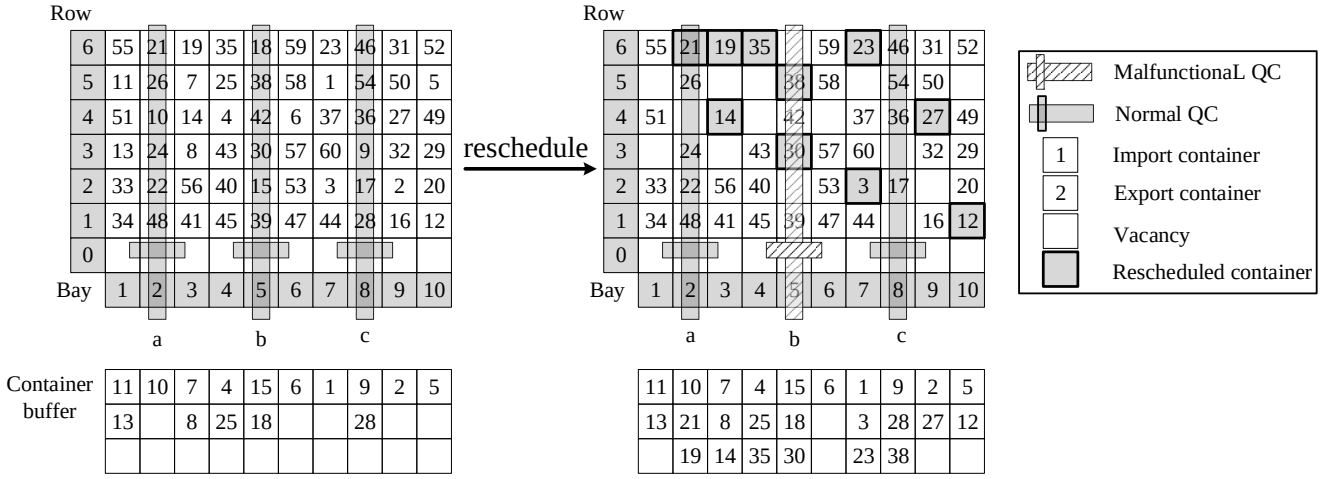

Figure 6. Schematic of the rescheduling mechanism.

5.1. Experiment Settings

This article applies the scenario of large-scale ship container loading and unloading to the experimental determination of genetic algorithm parameters, considering the task volume of a 368 m container ship. It can operate 10 QCs, which need to load 125 containers and unload 130 containers. Parameters of the proposed two-stage NSGA-II algorithm are established by testing various parameter combinations, whose results are shown in Figure 7. We categorize the results based on population scale, crossover rate, and mutation rate, and obtain the best values in the solution of the proposed algorithm. By comparing the optimal completion time of AGVs and the running time of the algorithm, we identify the optimal experimental parameters for the problem instance, which are the population size of 100, the crossover rate of 0.8, and the mutation rate of 0.1. Due to the lack of direct data on QCs fault, this study calculated the fault probability of QCs reasonably on the basis of the existing literature, and the remaining parameters were set based on previous studies as shown in Table 3.

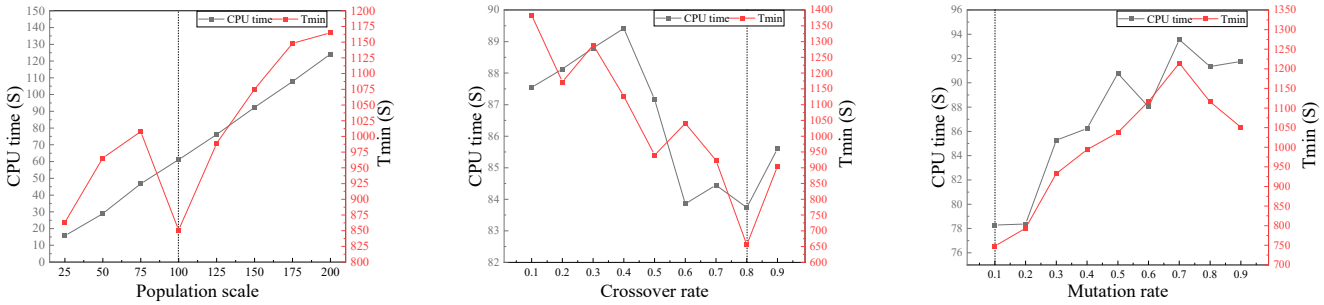

Figure 7. Effect of different parameters.

Table 3. Experimental parameter settings.

Parameter	Value	Parameter	Value	Parameter	Value
QC fault probability	0.03	t_2	1.28 min	b'	$b' = \begin{cases} \frac{0.001\%}{m}, AGVunlode \\ \frac{0.01\%}{m}, AGVoverlode \\ \frac{0.005\%}{s}, AGVwaiting \end{cases}$
v_1	2.5 m/s	t_3	1.08 min		
v_2	2.0 m/s	t_*	20 s		
t_1	1.08 min	b''	0.5 unit/s		

5.2. Numerical Analysis and Discussion

This article conducts a large-scale case study on a 368 m ship, examining the scheduling plan of the QCs under various loading and unloading modes. Additionally, it randomly generates the timing, sequence, and repair duration of QC faults by using a random number

list. By utilizing a fault scenario involving three QC faults with sequences 1, 2, and 8, as an example, the article analyzes the re-optimization efficiency of all operational QCs.

In Table 4, by analyzing the loading and unloading frequency of all QCs in single and dual cycle modes, optimization efficiency is calculated using Formula (22). In the normal scheduling plan, the average value of optimization efficiency is 22.968%, which means dual cycling loading and unloading mode increases the productivity of ACTs by an average of 22.968%. In the re-scheduling plan, the proposed algorithm still guarantees the average optimization efficiency of 22.926% in large-scale instances.

$$Optimization\ efficiency = \frac{N_2 \times (2t_1 - t_2)}{N_1 \times t_1} \tag{22}$$

Table 4. Normal scheduling plan of the QCs.

	Normal Scheduling Plan			Re-Scheduling Plan		
QC	**Single Cycling (N_1)**	**Dual Cycling (N_2)**	**Optimization Efficiency (%)**	**Single Cycling (N_1)**	**Dual Cycling (N_2)**	**Optimization Efficiency (%)**
1	19	5	21.44%	16	5	25.46%
2	37	12	26.43%	21	2	7.76%
3	22	4	14.81%	14	1	5.82%
4	17	5	23.97%	15	1	5.43%
5	37	13	28.63%	30	14	38.02%
6	18	5	22.63%	23	10	35.43%
7	18	5	22.63%	28	12	34.92%
8	19	5	21.44%	20	7	28.52%
9	35	12	27.94%	27	11	33.20%
10	33	8	19.75%	61	11	14.69%

In this paper, *GAP* provides a comparable numerical value, calculated as the effect of QCs faults on loading and unloading efficiency, as shown in Formula (23). In this fault scenario, ship loading and unloading time increased compared to the normal scheduling plan. In this large-scale instance, the overall optimal completion time (T') of the normal scheduling scheme is 2616.228 s, and the overall optimal completion time (T'') of the re-scheduling scheme is 3633.407 s. It is necessary to make rescheduling plans for the QC faults because QC faults decrease the ship loading and unloading efficiency by 38.880%. In addition, the proposed rescheduling scheme can still maintain the optimization efficiency of the QC dual cycling to be above 22.926%. The proposed algorithm remains effective even when dealing with large-scale instance calculation.

$$GAP = \frac{T'' - T'}{T'} \tag{23}$$

5.3. Algorithm Validity Verification Experiment

In this section, to further test the effectiveness of the proposed algorithm, randomly generated fault scenarios are applied to container ships of three scales. The detailed experiments are designed as follows: (1) The small-scale ships of 148 m and 199 m can allow up to four and five QCs to operate, which need to load 33 containers and unload 34 containers, respectively. (2) The medium-scale ships of 224 m and 299 m can allow up to six and eight QCs to operate at the same time, which need to load 60 containers and unload 118 containers, respectively. (3) The large-scale ships of 368 m can operate ten QCs, which need to load 125 containers and unload 130 containers.

During the process of these experiments, we ran the calculation examples of each scale five times and recorded the average results. We took the normal initial scheduling scheme with dual cycle mode by NSGA-II algorithm, namely baseline model, and randomly generated QC faults on this basis. Then, we compared the objective function values of two algorithms with normal dual cycle mode under QC faults, namely the proposed two-

stage NSGA-II algorithm and the traditional NSGA-II algorithm. "*GAP.Err*" and "*GAP.Imp*" are indicators used to compare algorithm performance. They refer to the calculation method of "*GAP*" as described in Formula (23). For their specific meanings, please refer to the notes in the table. To assess the performance of the Baseline model, NSGA-II and Two-stage NSGA-II on the same basis, the parameters were set the same as two-stage NSGA-II. Furthermore, we investigated the effects of QC faults on the efficiency of ship loading and unloading, as well as the effects of different fault states.

For large-scale ships, the loading and unloading efficiency with and without QC faults are given in Table 5. Five typical fault scenarios are selected based on the location and number of faulty QCs, and the simulation scenarios are shown in Appendix A. Specifically, QCs 1, 2, and 8 are faulty in scenario 1; QCs 4, 5, and 6 are faulty in scenario 2; QCs 1 and 7 are faulty in scenario 3; QC 4 is faulty in scenario 4; and QC 10 is faulty in scenario 5. According to the results of the experimental examples in Table 5, the handling time of ACTs under QC faults on large-scale ships increases by at least 38.5% and possibly up to 90.64%. The objective value of the proposed two-stage NSGA-II algorithm is obviously lower than that of the traditional NSGA-II algorithm and the proposed algorithm can save about 20% of time.

Table 5. Algorithm comparison results in large-scale ship scenarios.

Scenario Sequence	Length/Bay	Baseline Model (s)	NSGA-II (s)	Two-Stage NSGA-II (s)	*GAP.Err* (%)	*GAP.Imp* (%)
1	368/48	2616.23	4987.66	3633.41	90.64	27.15
2	368/48	3364.17	4659.24	3822.89	38.50	17.95
3	368/48	2836.93	4434.27	3458.07	56.31	22.02
4	368/48	3301.59	4584.57	3487.17	38.86	23.94
5	368/48	2409.31	4134.03	3184.13	71.59	22.98

"*GAP.Err*" is the relative increase value of the objective values obtained by NSGA-II in the fault scenarios relative to that of initial objective values. "*GAP.Imp*" represents the proportion of reduction in the relative objective values of NSGA-II by Two-stage NSGA-II.

For medium-scale ships, the loading and unloading efficiency with and without QC faults are given in Table 6. Five typical fault scenarios are selected based on the location and number of faulty QCs in 299 m and 224 m ships, respectively, and the simulation scenarios are shown in Appendix B. Specifically, QC 4 is faulty in scenario 1; QCs 2, 7 and 8 are faulty in scenario 2; QCs 3, 4 and 5 are faulty in scenario 3; QCs 1 and 7 are faulty in scenario 4; QC 1 is faulty in scenario 5; QCs 3 and 4 are faulty in scenario 6; QCs 1 and 5 are faulty in scenario 7; QC 4 is faulty in scenario 8; QC 6 is faulty in scenario 9; QCs 3, 4 and 5 are faulty in scenario 10. According to the results of the experimental examples in Table 6, the handling time of ACTs under QC faults on medium-scale ships increases by at least 35.57% and possibly up to 85.78%. The objective value of the proposed two-stage NSGA-II algorithm is obviously lower than that of the traditional NSGA-II algorithm and the proposed algorithm can save about 21% of time.

Table 6. Algorithm comparison results in medium-scale ship scenarios.

Scenario Sequence	Length/Bay	Baseline Model (s)	NSGA-II (s)	Two-Stage NSGA-II (s)	*GAP.Err* (%)	*GAP.Imp* (%)
1	299/40-1	2142.37	2960.47	2489.64	38.19	15.90
2	299/40-2	1810.41	3363.29	2947.83	85.78	12.35
3	299/40-3	2086.11	3165.11	2760.97	51.72	12.77
4	299/40-4	2033.31	3428.34	2693.91	68.61	21.42
5	299/40-5	1892.75	3184.72	2211.38	68.26	30.56
6	224/32-1	2195.13	3786.53	2712.37	72.50	28.37
7	224/32-2	2533.61	3859.98	2606.63	52.35	32.47
8	224/32-3	2176.04	3469.09	2560.76	59.42	26.18

Table 6. *Cont.*

Scenario Sequence	Length/Bay	Baseline Model (s)	NSGA-II (s)	Two-Stage NSGA-II (s)	*GAP.Err* (%)	*GAP.Imp* (%)
9	224/32-4	2160.44	3610.93	2561.41	67.14	29.07
10	224/32-5	2780.87	3770.00	3368.71	35.57	10.64

"*GAP.Err*" is the relative increase value of the objective values obtained by NSGA-II in the fault scenarios relative to that of initial objective values. "*GAP.Imp*" represents the proportion of reduction in the relative objective values of NSGA-II by Two-stage NSGA-II.

For small-scale ships, the loading and unloading efficiency with and without QC faults are given in Table 7. Five typical fault scenarios are selected based on the location and number of faulty QCs in 199 m and 148 m ships, respectively, and the simulation scenarios are shown in Appendix C. Specifically, QCs 1, 2, and 3 are faulty in scenario 1; QC 3 is faulty in scenario 2; QC 1 is faulty in scenario 3; QCs 3 and 5 are faulty in scenario 4; QCs 3 and 4 are faulty in scenario 5; QCs 1 and 3 are faulty in scenario 6; QCs 1 and 4 are faulty in scenario 7; QCs 1, 2, and 4 are faulty in scenario 8; QCs 2, 3, and 4 are faulty in scenario 9; QC 2 is faulty in scenario 10. According to the results of the experimental examples in Table 7, the handling time of ACTs under QC faults on small-scale ships increases by at least 30.61% and possibly up to 92.83%. The objective value of the proposed two-stage NSGA-II algorithm is obviously lower than that of the traditional NSGA-II algorithm and the proposed algorithm can save about 30% of time.

Table 7. Algorithm comparison results in small-scale ship scenarios.

Scenario Sequence	Length/Bay	Baseline Model (s)	NSGA-II (s)	Two-Stage NSGA-II (s)	*GAP.Err* (%)	*GAP.Imp* (%)
1	199/20-1	516.63	932.99	909.85	80.59	2.48
2	199/20-2	500.97	829.78	544.83	65.64	34.34
3	199/20-3	485.03	842.28	521.50	73.66	38.09
4	199/20-4	505.30	974.35	646.33	92.83	33.67
5	199/20-5	591.20	1094.26	935.99	85.09	14.46
6	148/16-1	786.30	1512.76	872.46	92.39	42.33
7	148/16-2	727.68	1267.69	779.14	74.21	38.54
8	148/16-3	899.30	1665.87	1061.13	85.24	36.30
9	148/16-4	1153.87	1507.11	1153.87	30.61	23.44
10	148/16-5	902.61	1359.19	743.77	50.58	45.28

"*GAP.Err*" is the relative increase value of the objective values obtained by NSGA-II in the fault scenarios relative to that of initial objective values. "*GAP.Imp*" represents the proportion of reduction in the relative objective values of NSGA-II by Two-stage NSGA-II.

5.4. Sensitivity Analysis of Ship Scale

The mean values of the objectives for the experiments mentioned above are shown in Table 8 and Figure 8. Figure 8a indicates the impact of QC faults on the loading and unloading efficiency of large-scale, medium-scale, and small-scale ships.

Table 8. Comparison results of different algorithms on ship scales.

Scale (m)	Quay Crane/Bay	Baseline Model-Obj.1 (s)	NSGA-II-Obj.2 (s)	Two-Stage NSGA-II-Obj.3 (s)	*GAP.Err* (%)	*GAP.Imp* (%)
148	4/16	893.95	1462.52	922.07	66.61	37.18
199	5/20	519.83	934.73	711.70	79.56	24.61
224	6/32	2369.22	3699.31	2761.98	57.40	25.35
299	8/40	1992.99	3220.39	2620.75	62.51	18.60
368	10/56	2905.65	4559.96	3517.13	59.18	22.81

"*GAP.Err*" is the relative increase value of the objective values obtained by NSGA-II in the fault scenarios relative to that of initial objective values. "*GAP.Imp*" represents the proportion of reduction in the relative objective values of NSGA-II by Two-stage NSGA-II.

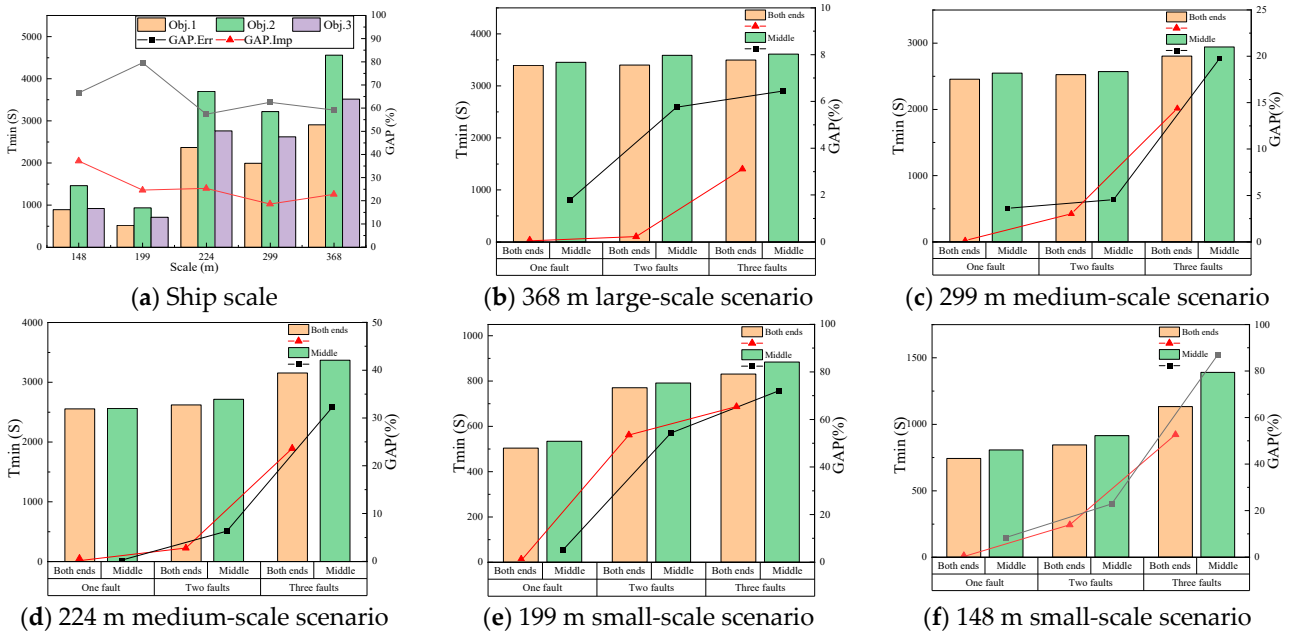

(**a**) Ship scale (**b**) 368 m large-scale scenario (**c**) 299 m medium-scale scenario

(**d**) 224 m medium-scale scenario (**e**) 199 m small-scale scenario (**f**) 148 m small-scale scenario

Figure 8. Influence statistics of ship scale, location, and number of faulty QCs.

It is observed that the productivity of small-scale ships is weakened with QC faults more than that of large-scale ships. Contrary to the NSGA-II algorithm, the two-stage NSGA-II algorithm exhibits a greater improvement in efficiency under QC faults in small-scale ships compared to large-scale ships. The effectiveness of the proposed two-stage NSGA-II algorithm is still significant and demonstrated its effect on the large-scale ship calculation.

5.5. Sensitivity Analysis of Location and Number of Faulty QCs

In addition to the ship scale, location and number of faulty QCs also affect the objective. In this study, we discuss the changes in the objective for various scenarios under different locations and numbers of faulty QCs. The fault scenarios above are calculated and compared according to the location and number of faulty QCs. The results are shown in Figure 8b–f. Under the condition of ensuring that the degree and number of faulty QC s in the same period are consistent, five fault scenario experiments were conducted for each period to obtain the average value. The experimental results of randomly generated QC fault scenarios with different fault locations and different fault numbers in the shipping schedule under five calculation case scales are statistically calculated. Taking the QC with a single fault and the fault location at both ends as the baseline, GAP values affected by fault location and fault number are calculated according to Formula (23) and represented as "*GAP.P*" and "*GAP.F*", respectively, as shown in Table 9.

Table 9. Comparison results of location and number of faulty QCs.

Number	Position	$\overline{Obj.}$ (s)	*GAP.P* (%)	*GAP.F* (%)		$\overline{GAP.P}$ (%)	$\overline{GAP.F}$ (%)
				Both Ends	Middle		
One fault	Both ends Middle	1930.35 1981.00	2.62	-	-	4.50	13.41
Two faults	Both ends Middle	2032.84 2115.92	4.09	5.31	6.81		
Three faults	Both ends Middle	2284.40 2439.78	6.80	18.34	23.16		

"*GAP.P*" is the influence degree of the location difference in the faulty QCs. "*GAP.F*" is the influence degree of the difference in the number of faulty QCs. $\overline{Obj.}$, $\overline{GAP.P}$, $\overline{GAP.F}$ are averages.

In general, the difference in objective function value is 4.5% for the location of faulty QCs and 13.41% for the number of faulty QCs. This indicates that the number of faulty QCs has a greater impact on loading and unloading efficiency than the actual location of faults. Under the same number of faulty QCs, the effect on loading and unloading efficiency of faulty QCs occurring at both ends of the ship is lower than that of faulty QCs occurring in the middle of the ship. During the loading and unloading period, the higher the number of faulty QCs, the greater the impact on efficiency.

6. Conclusions

This paper investigates an integrated scheduling problem of QCs, YCs, and AGVs considering QC faults, which is formulated as a mixed integer programming model. A rescheduling mechanism and integrated scheduling of handling equipment are accomplished simultaneously to minimize the loading and unloading time in this model. To solve the model, an adaptive two-stage NSGA-II algorithm is proposed, which first determines the range of adjacent operational QCs of the faulty QCs by comparing the horizontal distance between the operational QCs and the faulty QCs, and reallocates the unfinished container handling tasks of both the faulty QCs and their adjacent QCs, where the adjacent QCs of faulty QCs assume the container handling tasks. Then, the algorithm optimizes the task sequence of QCs, YCs, and AGVs according to scheduling rules.

Numerical experiments have been conducted on loading and unloading operation scenarios of three scale ships under different numbers and locations of faulty QCs and results show that the number of faulty QCs has a greater influence on the loading and unloading efficiency than their locations, and the impact of faulty QCs on the efficiency of small-scale ships is greater than that of large-scale ships, which indicate that the proposed algorithm can primely deal with the integrated scheduling problem of handling equipment considering QC faults while maintaining their dual cycling efficiency.

This paper analyzes the influence of QC faults on the integrated scheduling of handling equipment of ACTs and discusses the impact of the location and number of faulty QCs on efficiency. This article refers to the data of ACTs on the China Port Network to design and simulate a model for rescheduling the loading and unloading tasks of faulty QCs. The model can be applied to the customized rescheduling task of a ship QC faults in ACTs, and can demonstrate good results in various ship scales. However, the research hypothesis has certain limitations. It does not take into account the impact of other ships near the bay on the loading and unloading process, and it has not been validated for multiple ships loading and unloading scenarios along the entire coastline. In the future, we will discuss the integrated scheduling problem of handling equipment for multiple ships considering QC faults, and consider validating the algorithm using real data, to the extent possible.

Author Contributions: Conceptualization, T.L. and Q.D.; methodology, Q.D.; writing—original draft preparation, Q.D.; writing—review and editing, T.L. and Q.D.; visualization, X.S. All authors have read and agreed to the published version of the manuscript.

Funding: This work is supported by the Humanities and Social Sciences Foundation of the Ministry of Education under Grant 21YJC630066, National Natural Science Foundation of China under Grant 62173079 and U1808205.

Data Availability Statement: The data that support the findings of this study are available upon request from the corresponding author.

Conflicts of Interest: The authors declare no conflicts of interest.

Appendix A

Here, we present the normal scheduling plan and the rescheduling task of QCs in a large-scale scenario for a 368 m ship, as shown in Tables A1 and A2.

Table A1. Unfinished container sequence of the faulty QCs (a 368 m ship).

Normal Scheduling Plan	Scenario	Sequence of Faulty QCs	Sequence of Unfinished Containers
crane[1]=[34, 95, 59, 98, 22, 54, 45, 50, 3, 122, 47, 123, 118]	1	1	[122, 47, 123, 118]
crane[2]=[48, 104, 36, 7, 93, 107, 76, 117, 25, 90, 102, 100]		2	[102, 100]
crane[3]=[108, 6, 94, 56, 43, 124, 84, 113, 79, 75, 30, 26]		8	[63, 91, 73, 38, 23, 62, 81, 27, 115, 58, 112]
crane[4]=[35, 71, 40, 53, 13, 120, 88, 103, 69, 101, 4, 67, 52]	2	4	[67, 52]
crane[5]=[97, 86, 49, 61, 42, 99, 92, 114, 111, 64, 116, 18]		5	[49, 61, 42, 99, 92, 114, 111, 64, 116, 18]
crane[6]=[57, 39, 12, 77, 8, 68, 28, 105, 87, 17, 65, 46]		6	[17, 65, 46]
crane[7]=[29, 11, 66, 15, 44, 55, 10, 121, 78, 74, 16, 41, 5]	3	1	[22, 54, 45, 50, 3, 122, 47, 123, 118]
crane[8]=[83, 63, 91, 73, 38, 23, 62, 81, 27, 115, 58, 112]		7	[55, 10, 121, 78, 74, 16, 41, 5]
crane[9]=[1, 110, 109, 82, 33, 31, 60, 96, 32, 89, 37, 119, 70]	4	4	[69, 101, 4, 67, 52]
crane[10]=[72, 24, 9, 80, 2, 20, 51, 21, 19, 106, 85, 14, 125]	5	10	[80, 2, 20, 51, 21, 19, 106, 85, 14, 125]

Table A2. Results of each QC rescheduling task (a 368 m ship).

QC Sequence	Scenario 1	Scenario 2	Scenario 3	Scenario 4	Scenario 5
1		[92, 18]			
2			[22, 54, 50, 3, 122, 123, 118, 5]		
3	[102, 100]	[67, 52]	[45]	[69]	
4	[122, 47, 123, 118]		[47]		
5			[10]	[101, 4, 67]	
6		[49, 61, 42, 65]	[55, 121]	[52]	
7	[63, 91, 73, 38, 23, 81, 115, 58, 112]	[99, 17, 46, 114, 111, 64]			[85]
8		[116]	[78, 74, 16, 41]		
9	[62, 27]				[80, 2, 20, 51, 21, 19, 106, 14,125]
10					

Appendix B

Here, we present the normal scheduling plan and the rescheduling task of QCs in a medium-scale scenario for the 299 m and 224 m ships, as shown in Tables A3–A10.

Table A3. Unfinished container sequence of the faulty QCs (a 299 m ship).

Normal Scheduling Plan	Scenario	Sequence of Faulty QCs	Sequence of Unfinished Containers
crane[1]=[18, 33, 4, 15, 29, 30, 17]	1	4	[2, 32, 5, 31, 13, 14]
crane[2]=[23, 45, 49, 25, 16, 38, 26]	2	2	[25, 16, 38, 26]
crane[3]=[36, 27, 54, 11, 8, 20, 9]		7	[1, 41, 52, 39]
crane[4]=[60, 42, 2, 32, 5, 31, 13, 14]		8	[10, 21, 55]
crane[5]=[37, 50, 56, 57, 3, 46, 22, 51]	3	3	[27, 54, 11, 8, 20, 9]
crane[6]=[28, 59, 44, 12, 47, 34, 19, 6]		4	[13]
crane[7]=[35, 48, 24, 58, 1, 41, 52, 39]		5	[22, 51]
crane[8]=[43, 7, 40, 53, 10, 21, 55]	4	1	[15, 29, 30, 17]
		7	[52, 39]
	5	1	[15, 29, 30, 17]

Table A4. Results of each QC rescheduling task (a 299 m ship).

QC Sequence	Scenario 1	Scenario 2	Scenario 3	Scenario 4	Scenario 5
1		[25, 16, 38, 26]			
2	[14]		[27, 54, 11, 20, 9]	[15]	[15, 29]
3	[2, 32, 5, 31]			[29]	[30, 17]
4		[55]	[8]	[30]	
5	[13]	[39]	[13]		
6		[1, 10, 52, 21]	[22, 51]	[39]	
7					
8		[41]		[52, 17]	

Table A5. Unfinished container sequence of the faulty QCs (a 224 m ship).

Normal Scheduling Plan	Scenario	Sequence of Faulty QCs	Sequence of Unfinished Containers
crane[1]=[33, 18, 4, 15, 31, 25, 27, 17, 26, 60]	1	3	[54, 16, 30]
crane[2]=[23, 45, 38, 49, 11, 10, 57, 21, 43, 53]		4	[7, 41, 37, 13]
crane[3]=[9, 42, 36, 32, 14, 5, 2, 54, 16, 30]	2	1	[4, 15, 31, 25, 27, 17, 26, 60]
crane[4]=[8, 56, 3, 29, 50, 20, 7, 41, 37, 13]		5	[55, 44, 34, 1, 22, 19, 40, 46, 28]
crane[5]=[51, 55, 44, 34, 1, 22, 19, 40, 46, 28]	3	4	[7, 41, 37, 13]
crane[6]=[35, 24, 6, 48, 52, 47, 59, 39, 58, 12]	4	6	[47, 59, 39, 58, 12]
	5	3	[5, 2, 54, 16, 30]
		4	[7, 41, 37, 13]
		5	[40, 46, 28]

Table A6. Results of each QC rescheduling task (a 224 m ship).

QC Sequence	Scenario 1	Scenario 2	Scenario 3	Scenario 4	Scenario 5
1					
2	[54, 16,30]	[4, 15, 25, 17, 26, 60]			[54, 16, 30]
3	[37]	[55, 31]	[37, 13]	[12]	[13]
4		[44, 34, 22, 46, 28, 27]			[2, 46, 28, 37]
5	[7, 41, 13]		[7, 41]	[47, 59, 39, 58]	
6		[1, 19, 40]			[5, 40, 7, 41]

Appendix C

Here, we present the normal scheduling plan and the rescheduling task of QCs in a small-scale scenario for the 199 m and 148 m ships, as shown in Tables A7–A10.

Table A7. Unfinished container sequence of the faulty QCs (a 199 m ship).

Normal Scheduling Plan	Scenario	Sequence of Faulty QCs	Sequence of Unfinished Containers
crane[1]=[18, 33, 15, 4, 23, 8]	1	1	[4, 23, 8]
crane[2]=[16, 25, 26, 28, 2, 14, 3]		2	[2, 14, 3]
crane[3]=[27, 11, 19, 13, 5, 30]		3	[30]
crane[4]=[9, 32, 31, 10, 21, 17, 7]	2	3	[19, 13, 5, 30]
crane[5]=[6, 12, 20, 1, 22, 29, 24]	3	1	[23, 8]
	4	3	[13, 5, 30]
		5	[29, 24]
	5	3	[11, 19, 13, 5, 30]
		4	[32, 31, 10, 21, 17, 7]

Table A8. Results of each QC rescheduling task (a 199 m ship).

QC Sequence	Scenario 1	Scenario 2	Scenario 3	Scenario 4	Scenario 5
1					[19, 5, 30]
2		[13, 5, 30]	[8]	[5, 30]	[11, 13]
3					[32, 31]
4	[2, 4, 23]	[19]	[23]	[29, 24, 13]	
5	[30, 14, 3, 8]				[10, 21, 17, 7]

Table A9. Unfinished container sequence of the faulty QCs (a 148 m ship).

Normal Scheduling Plan	Scenario	Sequence of Faulty QCs	Sequence of Unfinished Containers
crane1=[16, 10, 12, 5, 6, 32, 3, 24]	1	1	[32, 3, 24]
crane2=[29, 21, 19, 27, 28, 18, 20, 25]		3	[31, 7, 13, 22, 4, 11]
crane3=[30, 14, 31, 7, 13, 22, 4, 11]	2	1	[32, 3, 24]
crane4=[26, 33, 1, 17, 15, 2, 9, 8, 23]		4	[1, 17, 15, 2, 9, 8, 23]
	3	1	[32, 3, 24]
		2	[25]
		4	[17, 15, 2, 9, 8, 23]
	4	2	[20, 25]
		3	[14, 31, 7, 13, 22, 4, 11]
		4	[33, 1, 17, 15, 2, 9, 8, 23]
	5	2	[18, 20, 25]

Table A10. Results of each QC rescheduling task (a 148 m ship).

QC Sequence	Scenario 1	Scenario 2	Scenario 3	Scenario 4	Scenario 5
1				[33, 20, 25, 31, 1, 7, 13, 17, 22, 4, 11, 15, 2, 9, 8, 23]	[20]
2	[32, 3, 24, 31, 7, 13]	[32, 3, 24]	[32, 3, 24]	[14]	
3		[1, 17, 15, 2, 9, 8, 23]	[17, 15, 2, 9, 8, 23,25]		[18, 25]
4	[22, 4, 11]				

References

1. Qiu, X.; Xu, G. Optimizing rail transport service in a dry port system. *IEEE Trans. Eng. Manag.* **2022**, *69*, 2670–2683. [CrossRef]
2. Knatz, G.; Notteboom, T.; Pallis, A.A. Container terminal automation: Revealing distinctive terminal characteristics and operating parameters. *Marit. Econ. Logist.* **2022**, *24*, 537–565. [CrossRef]
3. De, A.; Wang, J.; Tiwari, M.K. Hybridizing basic variable neighborhood search with particle swarm optimization for solving sustainable ship routing and bunker management problem. *IEEE Trans. Intell. Transp. Syst.* **2020**, *21*, 986–997. [CrossRef]
4. Bathke, H.; Münch, C.; von der Gracht, H.A.; Hartmann, E. Building resilience through foresight: The case of maritime container shipping firms. *IEEE Trans. Eng. Manag.* **2024**, *71*, 10534–10556. [CrossRef]
5. Wang, P.; Mileski, J.P.; Zeng, Q. Alignments between strategic content and process structure: The case of container terminal service process automation. *Marit. Econ. Logist.* **2019**, *21*, 543–558. [CrossRef]
6. Zhong, Z.L.; Guo, Y.Y.; Zhang, J.H.; Yang, S.X. Energy-aware integrated scheduling for container terminals with conflict-free AGVs. *J. Syst. Sci. Syst. Eng.* **2023**, *32*, 413–443. [CrossRef]
7. Dąbrowska, E. Monte carlo simulation based optimization of port grain trasportation system reliability. In Proceedings of the 2019 International Conference on Information and Digital Technologies (IDT), Zilina, Slovakia, 25–27 June 2019; pp. 86–91.
8. Zhang, X.; Li, H.; Sheu, J. Integrated scheduling optimization of AGV and double yard cranes in automated container terminals. *Transp. Res. Part B-Meth.* **2024**, *179*, 102871. [CrossRef]
9. Wang, M.; Zhou, C.; Wang, A. A cluster-based yard template design integrated with yard crane deployment using a placement heuristic. *Transp. Res. Part E-Log.* **2022**, *160*, 102657. [CrossRef]
10. Hang, Y.; Huang, M.; He, J.; Tan, C. The clustering strategy for stacks allocation in automated container terminals. *Marit. Policy Manag.* **2022**, *50*, 1102–1117.
11. Yang, Y.; Zhong, M.; Dessouky, Y.; Postolache, O. An integrated scheduling method for AGV routing in automated container terminals. *Comput. Ind. Eng.* **2018**, *126*, 482–493. [CrossRef]
12. Zhou, C.; Lee, B.K.; Li, H. Integrated optimization on yard crane scheduling and vehicle positioning at container yards. *Transp. Res. Part E-Log.* **2020**, *138*, 101966. [CrossRef]
13. Jiang, X.J.; Yang, X.M. A column generation approach for the crane scheduling with sidekick in a perpendicular automated yard block. *Transp. Res. Part E-Log.* **2023**, *176*, 103154. [CrossRef]
14. Tian, Y.; Zhou, Q.; Zhu, B.F. Integrated scheduling of dual-cycle AGV and yard crane at automated container terminal. *J. Tran. Sys. Eng.* **2020**, *20*, 216–243.
15. Tan, C.; Yan, W.; Yue, J. Quay crane scheduling in automated container terminal for the trade-off between operation efficiency and energy consumption. *Adv. Eng. Inf.* **2021**, *48*, 101285. [CrossRef]
16. Yang, X.; Hu, H.; Cheng, C.; Wang, Y. Automated guided vehicle (AGV) scheduling in automated container terminals (ACTs) focusing on battery swapping and speed control. *J. Mar. Sci. Eng.* **2023**, *11*, 1852. [CrossRef]
17. Song, X.; Chen, N.; Zhao, M.; Wu, Q.; Liao, Q.; Ye, J. Novel AGV resilient scheduling for automated container terminals considering charging strategy. *Ocean Coast. Manag.* **2024**, *250*, 107014. [CrossRef]

18. De, A.; Wang, J.; Tiwari, M.K. Fuel bunker management strategies within sustainable container shipping operation considering disruption and recovery policies. *IEEE Trans. Eng. Manag.* **2021**, *68*, 1089–1111. [CrossRef]
19. De, A.; Choudhary, A.; Tiwari, K.M. Multiobjective approach for sustainable ship routing and scheduling with draft restrictions. *IEEE Trans. Eng. Manag.* **2019**, *66*, 35–51. [CrossRef]
20. Li, L.; Li, Y.; Liu, R.; Zhou, Y.; Pan, E. A two-stage stochastic programming for AGV scheduling with random tasks and battery swapping in automated container terminals. *Transp. Res. Part E-Log.* **2023**, *174*, 103110. [CrossRef]
21. Xing, Z.; Liu, H.; Wang, T.; Chew, E.P.; Lee, L.H.; Tan, K.C. Integrated automated guided vehicle dispatching and equipment scheduling with speed optimization. *Transp. Res. Part E-Log.* **2023**, *169*, 102993. [CrossRef]
22. Li, X.; Peng, Y.; Tian, Q.; Feng, T.; Wang, W.; Cao, Z.; Song, X. A decomposition-based optimization method for integrated vehicle charging and operation scheduling in automated container terminals under fast charging technology. *Transp. Res. Part E-Log.* **2023**, *180*, 103338. [CrossRef]
23. Klerides, E.; Hadjiconstantinou, E. Modelling and solution approaches to the multi-load AGV dispatching problem in container terminals. *Marit. Econ. Logist.* **2011**, *13*, 371–386. [CrossRef]
24. Chen, X.; He, S.; Zhang, Y.; Tong, L.; Shang, P.; Zhou, X. Yard crane and AGV scheduling in automated container terminal: A multi-robot task allocation framework. *Transp. Res. Part C Emerg. Technol.* **2020**, *114*, 241–271. [CrossRef]
25. Huang, C.; Zhang, R. Container drayage transportation scheduling with foldable and standard containers. *IEEE Trans. Eng. Manag.* **2023**, *70*, 3497–3511. [CrossRef]
26. Xu, B.; Jie, D.; Li, J.; Yang, Y.; Wen, F.; Song, H. Integrated scheduling optimization of U-shaped automated container terminal under loading and unloading mode. *Comput. Ind. Eng.* **2021**, *162*, 107695. [CrossRef]
27. Zheng, X.; Liang, C.; Wang, Y.; Shi, J.; Lim, G. Multi-AGV dynamic scheduling in an automated container terminal: A deep reinforcement learning approach. *Mathematics* **2022**, *10*, 4575. [CrossRef]
28. Darius, D.; Mindaugas, K.; Audrius, S. Deep reinforcement learning based optimization of automated guided vehicle time and energy consumption in a container terminal. *Alex. Eng. J.* **2023**, *67*, 397–407.
29. Weerasinghe, B.A.; Perera, H.N.; Bai, X. Optimizing container terminal operations: A systematic review of operations research applications. *Marit. Econ. Logist.* **2023**, *26*, 307–341. [CrossRef]
30. Yang, Y.; Sun, S.; He, S.; Jiang, Y.; Wang, X.; Yin, H.; Zhu, J. Research on the multi-equipment cooperative scheduling method of sea-rail automated container terminals under the loading and unloading mode. *J. Mar. Sci. Eng.* **2023**, *11*, 1975. [CrossRef]
31. Zheng, H.; Wang, Z.; Zhu, X. Multi-stage rescheduling decision of container terminal quay crane considering the fault. *Syst. Eng. The. Pra.* **2021**, *41*, 3321–3335.
32. Kaliszewski, A.; Kozłowski, A.; Dąbrowski, J.; Klimek, H. Linkedin survey reveals competitiveness factors of container terminals: Forwarders' view. *Transp. Policy* **2021**, *106*, 131–140. [CrossRef]
33. Qi, J.; Zheng, J.; Yang, L.; Fan, Y. Impact analysis of different container arrival patterns on ship scheduling in liner shipping. *Marit. Policy Manag.* **2020**, *48*, 331–353. [CrossRef]
34. Zheng, F.F.; Li, Y.; Chu, F.; Liu, M.; Xu, Y.F. Integrated berth allocation and quay crane assignment with maintenance activities. *Int. J. Prod. Res.* **2018**, *57*, 3478–3503. [CrossRef]
35. Chargui, K.; Zouadi, T.; Sreedharan, V.R.; Fallahi, A.E.; Reghioui, M. A novel proactive–reactive scheduling approach for the quay crane scheduling problem: A VUCA perspective. *IEEE Trans. Eng. Manag.* **2023**, *70*, 2594–2607. [CrossRef]
36. Rajali, J.M.; Saman, A.K.A.; Abdul, H.M.F.; Siang, K.H. A stochastic petri net-based approach for operational performance estimation of quay cranes. *Qual. Reliab. Eng. Int.* **2023**, *39*, 1660–1680.
37. Duan, Y.; Ren, H.; Xu, F.; Yang, X.; Meng, Y. Bi-objective integrated scheduling of quay cranes and automated guided vehicles. *J. Mar. Sci. Eng.* **2023**, *11*, 1492. [CrossRef]
38. Sun, B.; Zhai, G.; Li, S.; Pei, B. Multi-resource collaborative scheduling problem of automated terminal considering the AGV charging effect under COVID-19. *Ocean Coast. Manag.* **2023**, *232*, 106422. [CrossRef]
39. Li, S.; Wang, N.; Jia, T.; He, Z.; Liang, H. Multiobjective optimization for multiperiod reverse logistics network design. *IEEE Trans. Eng. Manag.* **2016**, *63*, 223–236. [CrossRef]
40. Chen, C.; Hu, Z.; Wang, L. Scheduling of AGVs in automated container terminal based on the deep deterministic policy gradient (DDPG) using the convolutional neural network (CNN). *J. Mar. Sci. Eng.* **2021**, *9*, 1439. [CrossRef]
41. Ji, S.; Luan, D.; Chen, Z.; Guo, D. Integrated scheduling in automated container terminals considering AGV conflict-free routing. *Transp. Lett.* **2020**, *13*, 501–513.